A NON-LINEAR FILTERING ALGORITHM FOR THE MEASUREMENT OF RAINFALL DROP SIZE DISTRIBUTION

Takis Kasparis and John Lane
Department of Electrical and Computer Engineering
University of Central Florida
Orlando, FL 32816, USA
e-mail: tnk@ece.engr.ucf.edu

ABSTRACT

Using an impulse suppression algorithm, environmental noise such as thunder and wind can be filtered from the sound of raindrops impacting an acoustic rain gauge sensor. A non-linear filter algorithm, based on a gated median filter, was previously used to suppress scratch noise from damaged phonograph records. The goal of this work is to adapt this impulse suppression algorithm and evaluate its performance in detecting and filtering the impulse signal from a sensor element of the Acoustic Rain Gauge Array at the University of Central Florida. In this case, the amplitude of each impulse is a measurement of the raindrop size impacting the sensor. By subtracting the filtered signal from a delayed version of the original, the output signal contains only the drop impulses from which the raindrop size distribution can be derived.

INTRODUCTION

Partially spurred by the advent of radar, an extensive amount of experimental and theoretical work was performed during the 1940's to analyze rainfall. The main thrust of that research was to describe and characterize rain as a volume density distribution of water droplets, where the number of drops in a volume of air as a function of drop size is defined as the drop size distribution (DSD). Since that time, interest in characterizing rain from this perspective has continued. Weather radar remains the primary motivation in rainfall DSD measurements, since in this case, the quantity of interest is radar reflectivity, the 6th moment of the DSD. Other important quantities can be extracted from the DSD, as described in the following sections.

Impact disdrometers are the class of rainfall measurement instruments that record individual raindrop impacts. These instruments convert the impact of a single water drop at terminal velocity to an electrical impulse. The disdrometer's processing electronics is responsible for converting the impulse amplitude to an equivalent drop diameter. The relationship between electrical signal amplitude and drop diameter is dependent on the various physical mechanisms which couple the drop momentum or impulsive force (Becker, 1954) to the mechanical portion of the sensing element (Joss, 1976). Most impact disdrometers transform drop momentum to an electrical output by a direct coupling of the sensor mass to the sensor transducer (Rowland, 1976). These instruments can be modeled as a simple spring-mass system where the sensor mass reacts to the impulsive force of the drop impact. The sensing element of the Acoustic Rain Gauge Array (ARGA), is similar in principle to previous impact disdrometers except that in this case, the drop impact impulse is acoustically coupled through air to the transducer (Lane, 1997).

RAIN DROP SIZE DISTRIBUTION

The DSD is a fundamental quantity which is very useful in describing the various physical characteristics of rainfall. A simple but very popular approximation for the DSD is the Marshall-Palmer (MP) distribution (Marshall, 1948):

$$N(D) = N_0 e^{\lambda D} \qquad (1a)$$

$$\lambda = \zeta R^{-\varepsilon} \qquad (1b)$$

where values in Equations (1a) and (1b) have been experimentally measured as $N_0 \approx 8000$ [m^{-3} mm^{-1}], $\varepsilon \approx 0.21$, and $\lambda \approx 41R^{-0.21}$ [cm^{-1}] with R expressed in [mm/hr].

The number of drops as a function of drop size which exit or enter a unit volume of air is called the flux density of

rain. This quantity is experimentally measured as the number of drops versus diameter that strike a horizontal surface:

$$n(D) = v_D N(D) \tag{2a}$$

where v_D is the drop velocity. To a good approximation, all rain drops that strike a horizontal surface on the ground can be considered to be traveling at a terminal velocity. Figure 1 shows that the relationship between terminal velocity and drop diameter can be approximated by a simple formula (Gunn, 1948):

$$v_D \approx KD^{1/2} \tag{2b}$$

where $K \approx 1420$ [$cm^{1/2}$ s^{-1}]. Combining Equations (2a) and (2b) yields:

$$n(D) \approx KD^{1/2}N(D) \tag{2c}$$

The rainfall rate distribution is the product of the drop volume and flux density distribution, where a spherical drop volume is assumed (even though drops at terminal velocity tend to be more elliptical due to the frictional drag of air):

$$R(D) = V_D n(D) \tag{3a}$$

$$V_D = \frac{\pi}{6} D^3 \tag{3b}$$

$$R(D) = \frac{\pi}{6} K D^{7/2} N(D) \tag{3c}$$

The total rainfall rate R is just the integral of $R(D)$ over all possible diameters (R is the quantity measured by a rain gauge):

$$R = \int_0^\infty R(D)dD \tag{4a}$$

$$= \frac{\pi}{6} K N_0 \Gamma(9/2) \lambda^{-9/2} \tag{4b}$$

$$= \frac{\pi}{6} K N_0 \Gamma(9/2) \zeta^{-9/2} R \tag{4c}$$

where $\varepsilon \approx 2/9$, so that:

$$N_0 = \frac{6\zeta^{9/2}}{\pi K \Gamma(9/2)} \tag{5a}$$

Since K and ζ are in different units, a conversion factor is needed in Equation (5a) so that the original mixed set of units may be used:

$$N_0 = \left(\frac{10^4}{3600}\right) \frac{6\zeta^{9/2}}{\pi K \Gamma(9/2)} \quad [m^{-3} mm^{-1}] \tag{5b}$$

If ζ =41 is used in Equation (5b), then $N_0 \approx 5810$ [m^{-3} mm^{-1}], which is in fair agreement with that observed experimentally.

Many useful physical properties of rainfall are found to be moments of the DSD (Nystuen, 1996):

$$M_x = \int_0^\infty D^x N(D)dD \tag{6}$$

M_0 is number of drops per unit volume, M_3 is the volume of water per unit volume, $M_{7/2}$ is the total rainfall rate, and M_6 is radar reflectivity (the physical quantity measure by weather radar).

ADAPTIVE SCRATCH NOISE FILTER

The adaptive scratch noise filter (Kasparis, 1993) was originally inspired from the similarities between scratch filtering of damaged phonograph records and suppression of impulsive noise (known as "salt and pepper") from images. This suggested the idea that filters traditionally used in image processing could be applied for scratch filtering as well. A well-known filter for salt and pepper noise suppression is the median filter (MF) which replaces each image pixel with the median of surrounding pixels. However, direct median filtering has undesirable side-effects such as smoothing of noise free regions, resulting in loss of image detail. The conditional median filter (CMF) improves the performance of the MF by selectively filtering only pixels contaminated by impulses. Scratch impulses in audio signals have some distinct differences from salt and pepper impulses in images, thus direct application of filters such as the CMF may not produce satisfactory results. This stems from the nature of the source that generates the impulses. Salt and pepper noise is generated from bit errors in the data stream and occurs as isolated impulses. Scratch noise is generated when a phonograph playback stylus encounters discontinuities in the groove and is essentially the impulse response of the playback mechanism. A typical scratch wave-form consists of an initial pulse followed by decaying oscillations, due to mechanical vibration of the stylus.

In the case of rainfall drop measurements, the waveforms have a very similar appearance, but now the role of signal and noise is reversed. As shown in the top trace of Figure 3, the drop impact is the equivalent of the phonograph scratch, while thunder is the equivalent of the music audio signal.

The gated median filter (GMF) is a modification of the CMF algorithm where a independent detector first locates impulses, then gates a median filter on and off accordingly, as shown in the block diagram of Figure 2. Impulse suppression is accomplished with a median filter (MF) placed in the main signal path. The MF is normally disabled and bypassed, except in those signal regions where impulses have been detected, i.e.:

$$y_n = \begin{Bmatrix} m_n & \text{if} \quad g_n > 0 \\ x_n & otherwise \end{Bmatrix} \tag{7a}$$

where:

$$m_n = med\{x_{n-k} \ldots x_n, \ldots x_{n+k}\} \tag{7b}$$

is the median value over a window of length $N = 2k + 1$ samples. x_n and y_n are the input and output sequences and g_n is a gating signal which is provided with the correct timing so that the MF is activated when impulses are within the filter window. It is well known that MFs preserve smooth signal regions and suppress impulses of widths narrower than $k = (N\text{-}1)/2$. The signal g_n is generated in the lower branch of Figure 2 where impulse detection and gating generation take place.

The input signal is first high-pass filtered so that the presence of impulses (which are rich in high frequencies) are enhanced. The high-pass filter used is a simple discrete second derivative approximation, and the output z_n is given by:

$$z_n = D^2\{x_n\} = x_{n-1} - 2x_n + x_{n+1} \tag{8}$$

The second derivative produces a large output when an abrupt change in slope is encountered. Because of the oscillatory characteristics of the scratch wave-form, the MF must remain active for the entire duration of a scratch. Thus, the gating impulse must bracket the scratch wave form. An impulse profile w_n can be obtained from the envelope of a full-wave rectified z_n. This can be accomplished by a local RMS operator applied on z_n over a sliding window of length M, i.e.:

$$w_n = \left[\frac{1}{M+1} \sum_{j=-M/2}^{M/2} z_{n+j}^2 \right]^{1/2} \tag{9}$$

This RMS operator was found to discriminate impulses better than simple local averaging of $|z_n|$. Smoothing the output of the high-pass filter defines the impulse duration more clearly. The length M of the averaging window is not very critical, but it should be large enough to include at least one cycle of the impulsive oscillations.

The gating signal g_n can be obtained by applying a threshold on w_n with respect to a signal reference floor b_n which excludes peak excursions. Again, we may call upon the MF for assistance in generating b_n but a recursive median filter (RMF) would be more appropriate because in a single application it can suppress multiple closely spaced impulses whereas the MF may require repeated applications. The RMF is identical to the MF with the exception that previous medians are placed in the input buffer and used in the computation of' subsequent medians. Compared to Equation (7a) the RMF output r_n is obtained from:

$$r_n = med\{r_{n-k} \ldots, r_{n-1}, x_n, x_{n+1}, \ldots x_{n+k}\} \tag{10}$$

Since impulse peak widths in w_n may exceed 30 samples, the RMF window length required to extract the background should be over 60 samples, but such large windows are computationally expensive. A simple method to reduce the window size and number of computations, without significant performance loss, is to decimate w_n and use a small RMF window. The final background extraction operator, in this case, can be written as:

$$b_n = RMF\{w_n; L, K\} \tag{11}$$

where L is the RMF window length, K is the decimation ratio, and KL is the effective RMF window length. The gating signal is defined from the normalized absolute difference between w_n and b_n as:

$$g_n = \begin{Bmatrix} m & \text{if} \quad d_n > C \\ 0 & \text{otherwise} \end{Bmatrix} \tag{12a}$$

where

$$d_n = \frac{|w_n - b_n|}{b_n} \tag{12b}$$

and m is the number of consecutive sample positions where the upper branch of Equation (12a) is valid. Essentially m indicates the width of the resulting gates in g_n. Normalization by b_n makes d_n insensitive to input conditions (amplitude or spectral content) so that a constant value for the threshold C can be used. Values of C from 1.5 to 2.5 seemed to work well over a wide range of input conditions.

The adaptive scratch filter can be expressed as:

$$y_n = med\{x_{n-g_n} \ldots x_n, \ldots x_{n+g_n}\} \tag{13}$$

where the filter window length N_n=2g_n+1 is dependent on the gate width so that when g_n=O, no filtering takes place. For this reason, the filter is adaptive. The top trace of Figure 3 x_n shows typical rain drop data from an ARGA sensor contaminated by thunder and wind noise. The middle trace y_n is the result of filtering x_n with the filter algorithm summarized in Equation (13). The final data used to determine the drop size distribution (DSD), shown in the bottom trace of Figure 3, is simply x_n-y_n.

ACOUSTIC DISDROMETER OUTPUT DISPLAY

The primary DSP functions previously used to process data from the ARGA disdrometer, are signal (1) filtering and (2) peak detection and amplitude estimation. The filtering is accomplished by a 16th order bandpass filter, centered around the resonant frequency of the sensor diaphragm, f_0=750 Hz, with a bandwidth of 350 Hz. An amplitude estimation algorithm incorporates any necessary dead-time by recognizing characteristics in the pulse which may correspond to impulse overlap. The peak detection and amplitude estimation algorithms are based on pattern recognition principles.

During a rainfall event, all impulses over the sensor's measurement area, and within a time frame interval T (for example, T=30 seconds), are measured and converted to equivalent drop volumes using a parametric relationship between drop diameter and the maximum amplitude of the measured impulse (Lane, 1997). The most direct output display mode of the acoustic disdrometer is drop size versus time (D/t) plot, as shown in Figure 4a. This output format is accomplished by plotting a small dot at the corresponding drop diameter (vertical axis) and time (horizontal axis) coordinate, where each dot represents a measured raindrop (McFarquhar, 1996). A complex plotting routine might adjust the dot size based on the raindrop diameter in order to accurately convey the drop density. In Figure 4a, all dots are of equal size, but the density is never-the-less apparent from this plotting format. Consecutive vertical time slices of the D/t plot can be readily converted to a rainfall rate versus diameter $R(D)$ distribution (or histogram) by counting the number of dots in corresponding drop size bins, converting to equivalent spherical volumes, dividing out the area of the sensor, and dividing by the width of the time slice. The total rainfall rate R during that time interval is the integral of $R(D)$ over all diameters. Figure 4b shows R as a function of time corresponding to the data in Figure 4a. The dotted line is rainfall rate measured by a tipping bucket rain gauge. The data shown in Figure 4 was processed by the bandpass filter method described in a previous section.

RESULTS AND DISCUSSION

As can be seen by examination of the D/t plot of Figure 4a, linear filtering methods lead to problems during high background noise, such as thunder shown as vertical lines, which degrade the overall DSD measurement. Figure 5a and 5b show the same data as Figures 4, but processed by the adaptive non-linear filter described by Equation (13). The thunder noise is suppressed in this case. However, the lower drop size detection limit has increased so that in this case of Figure 5a, the DSD lower cutoff is approximately 2 mm, whereas in the previous case, data is detected to approximately 1 mm or lower.

Optimization of the median filter parameters could increase the drop diameter sensitivity, with a possible trade-off with some noise contamination. Alternatively, a method which may yield the best performance would be a combination of both the linear and non-linear filtering methods. A possible strategy would be to use linear filtering on data with relatively low background noise, then automatically switch to the non-linear filter when the background noise rises above a threshold value. This will be a subject of future work.

REFERENCES

R. B. Becker, Introduction to Theoretical Mechanics, McGraw-Hill Book Company, New York, NY, pp. 173-174, 1954.

R. Gunn and G. D. Kinzer, "The Terminal Velocity of Fall for Water Droplets in Stagnant Air," Journal of Applied Meteorology, Vol. 6, pp. 243-248, 1948.

J. Joss and A. Waldvogel, "Comments on "Some Observation on the Joss-Waldvogel Rainfall Disdrometer"," Journal of Applied Meteorology, Vol. 16, pp. 112-113, January 1976.

T. Kasparis and J. Lane, "Adaptive Scratch Noise Filtering," IEEE Transactions on Consumer Electronics, Vol. 39, No. 4, pp. 917-922, November 1993.

J. Lane, T. Kasparis, and G. McFarquhar, "Acoustic Rain Gauge Array Experiment: Phase I," presented at the ERIM 4th International Conference on Remote Sensing for Marine and Coastal Environments, 17-19 March 1997, Orlando, FL, session G-25.

J. S. Marshall and W. M. Palmer, "The Distribution of Raindrops with Size," Journal of Meteorology, Vol. 9, pp. 327-332, 1948.

G. M. McFarquhar, "Flux Measurements of Pulsating Rain with a Disdrometer and Doppler Radar during Phase II of the Joint Tropical Rain Experiment in Malaysia," Journal of Applied Meteorology, Vol. 35, No. 6, pp. 859-874, June 1996.

J. A. Nystuen, "Acoustical Rainfall Analysis: Rainfall Drop Size Distribution Using the Underwater Sound Field," Journal of Atmospheric and Oceanic Technology, Vol. 13, pp. 74-84, February 1996.

J. R. Rowland, "Comparison of Two Different Raindrop Disdrometers." In 17th Radar Meteorology Conference, American Meteorological Society, Seattle, pp. 398-405, October, 1976.

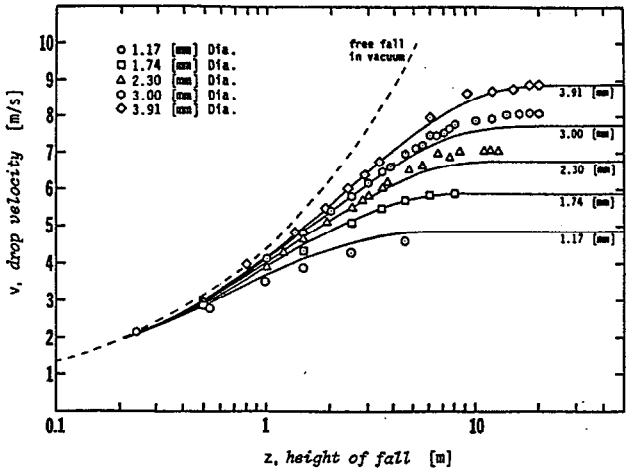

Figure 1. Water Drop Velocity Versus Fall Height for Various Drop Diameters.

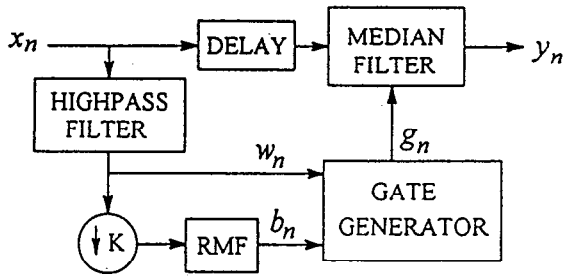

Figure 2. Block Diagram of Adaptive Scratch Filter

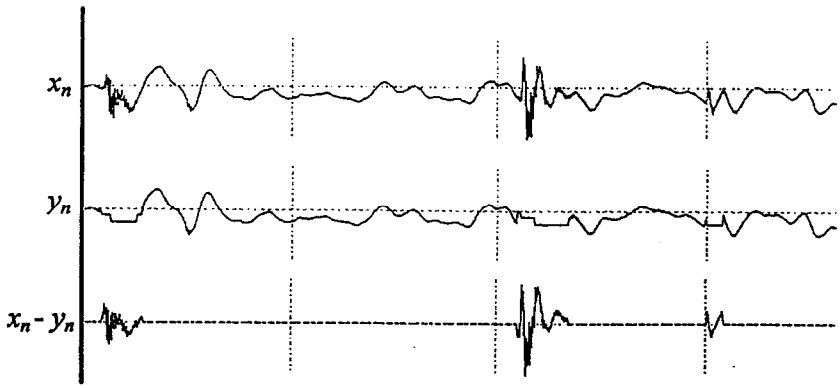

Figure 3. Processing of ARGA Disdrometer Data by Adaptive Scratch Filter Algorithm. Top Trace is Input Data, x_n; Middle Trace is Filter Output, y_n, as Described by Equation (13); and Bottom Trace is the Difference of the Input and Output Signals.

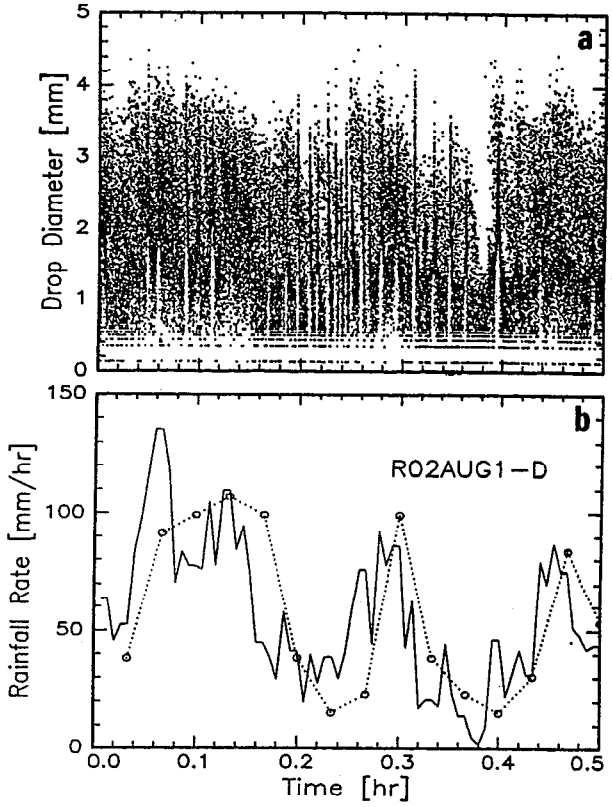

Figure 4. ARGA Disdrometer Data Processed by Previous Linear Filter. (a) Drop Diameter versus Time and (b) Calculated Rainfall Rate R versus Time (solid line) and Tipping Bucket Data (dotted line)

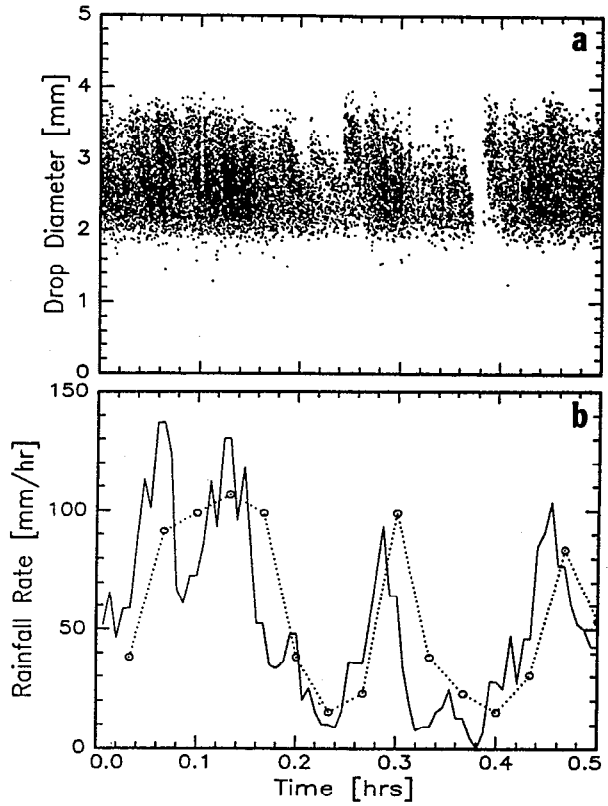

Figure 5. Same Data Shown in Figures 4, but Processed by Non-Linear Filter of Equation (13).